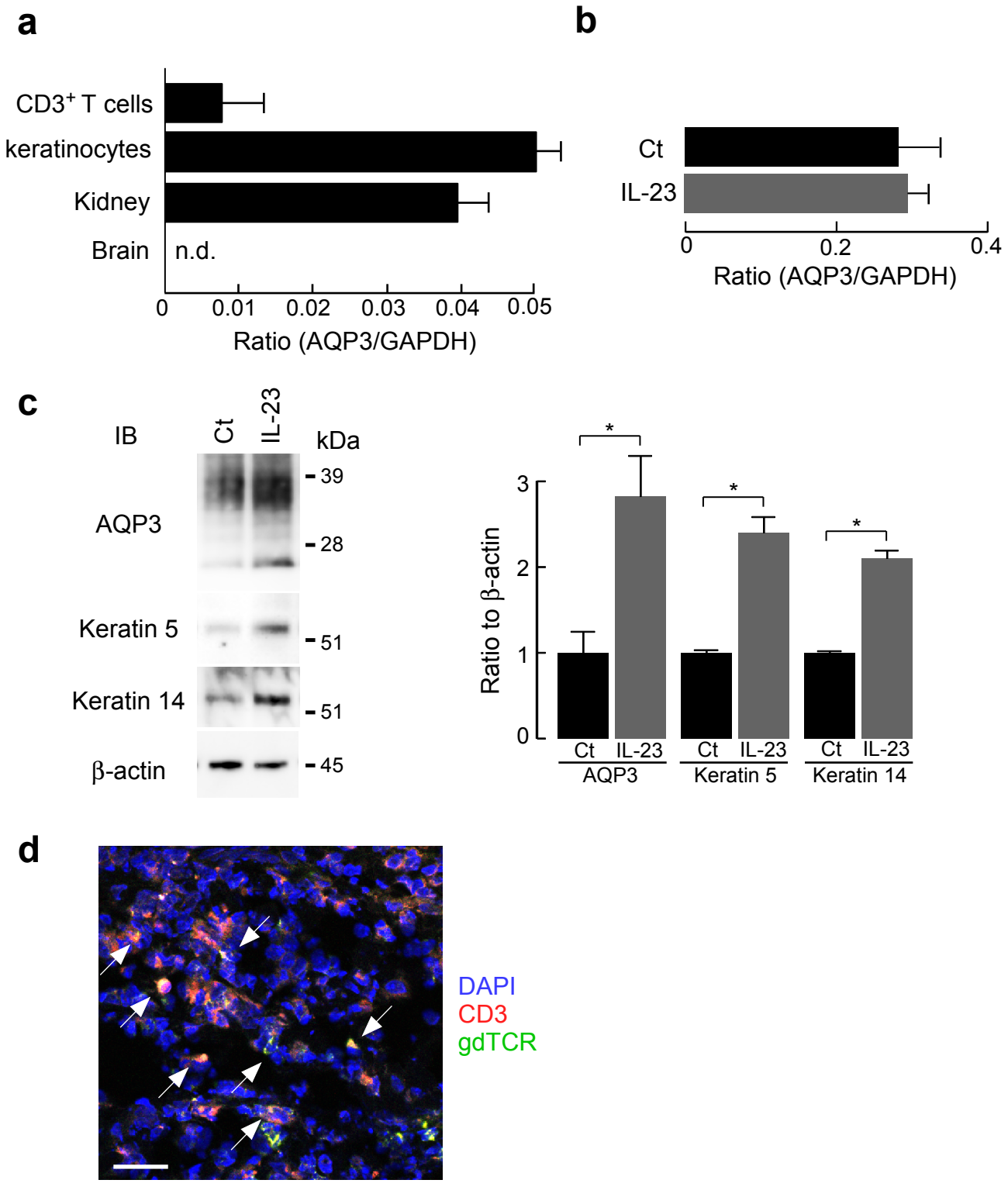

Supplementary Figure 1

a. AQP3 mRNA expression in sorted $CD3^+$ T cells, primary keratinocytes, kidney and brain tissues from C57BL/6 WT mice was measured by real-time RT-PCR. Data are expressed as the AQP3/GAPDH ratio (SE; n=3). **b-d.** IL-23 (500 ng) or vehicle control (PBS) were injected daily into the ear skin intradermally of WT mice for 4 days. **b.** AQP3 mRNA expression in epidermal cells from control and IL-23 treated skin (SE; n=6). **c.** (left) Representative immunoblot of epidermal homogenates with anti-AQP3, keratin 5, keratin 14, or β-actin antibodies. (right) Data are expressed as the indicated protein/β-actin ratio (SE, n=4, *$p < 0.01$). **d.** Representative immunostaining with anti-CD3 and γδTCR antibodies in WT mouse skin following IL-23 treatment (red; CD3, green; γδTCR, blue; DAPI). Bar, 50μm. Arrow; $CD3^+$ $γδTCR^+$ cell.

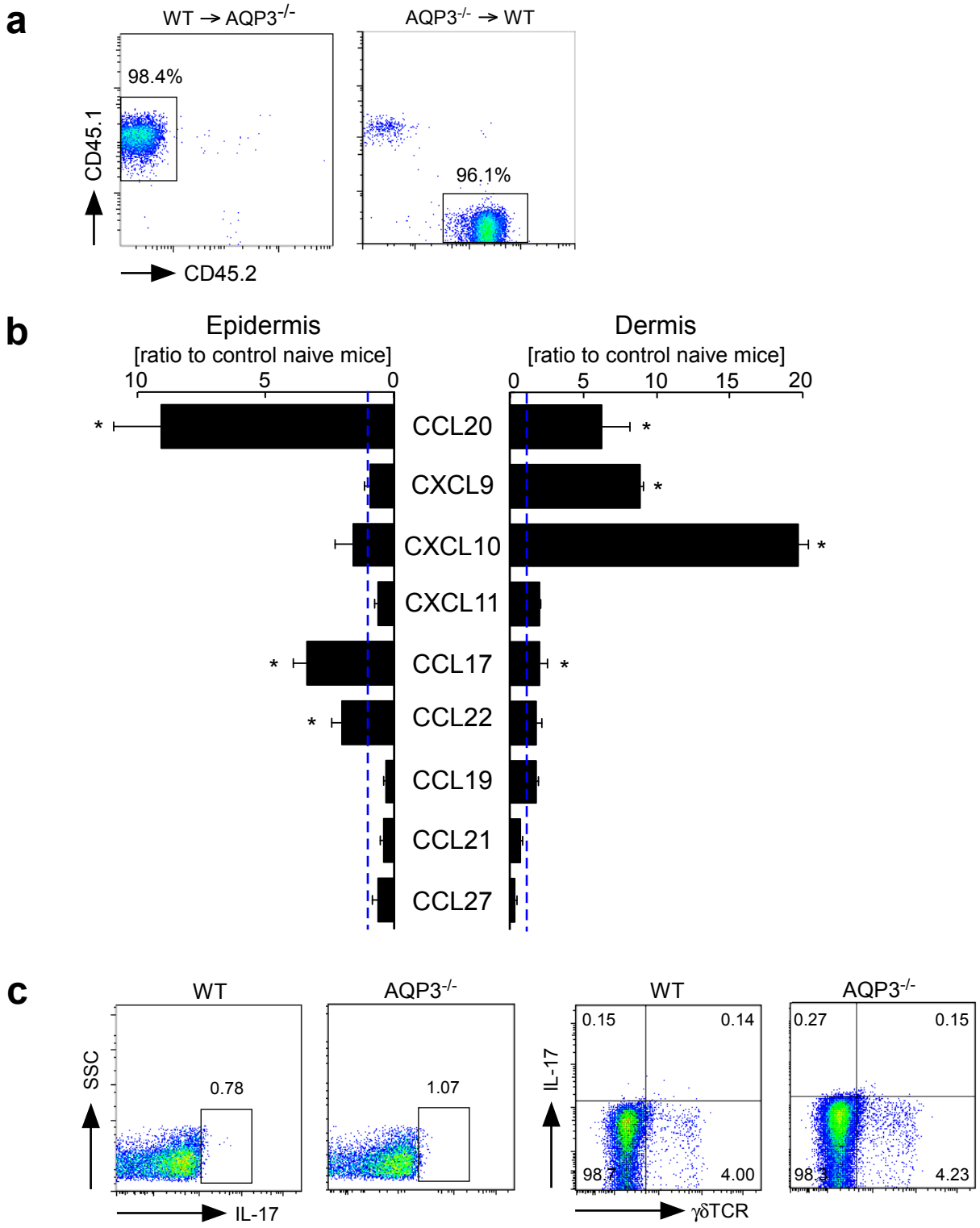

Supplementary Figure 2

a. Mice (WT or AQP3$^{-/-}$, 8-10 weeks old) were gamma-irradiated with two doses of 600rad, 3 hours apart. The irradiated mice received intravenous injection of bone marrow from WT or AQP3$^{-/-}$ mice. The chimerism was checked using C57BL/6 CD45.1 congenic mice. 60 days after of bone marrow transfer spleen cells were stained with CD45.1-pacific blue and CD45.2-APC, and analyzed by FACS. More than 95% cells of the recipient cells were replaced by donor cells. **b.** IL-23 (500 ng) or vehicle control (PBS) was daily intradermally injected into the ear skin of WT and AQP3$^{-/-}$ mice for 4 days. The skin samples were excised at 24 hours after the final IL-23 application. The mRNA was extracted from separated epidermis and dermis, and analyzed by quantitative RT-PCR. The expression levels of chemokines in epidermis and dermis of IL-23-treated WT skin. The relative expression ratio is calculated as the mRNA levels in IL-23 applied skin to vehicle control skin (SE, n=5, *p < 0.01, IL-23-treated skin *vs.* control skin by t-test). **c.** Skin-draining lymph node cells from IL-23-treated mice were stimulated with IL-23, and intracellular IL-17 expression was determined by flow cytometry. Left panels are representative dot plots gated on the total cells. The right panels are representative dot plots gated on the CD3^{+} T cells.

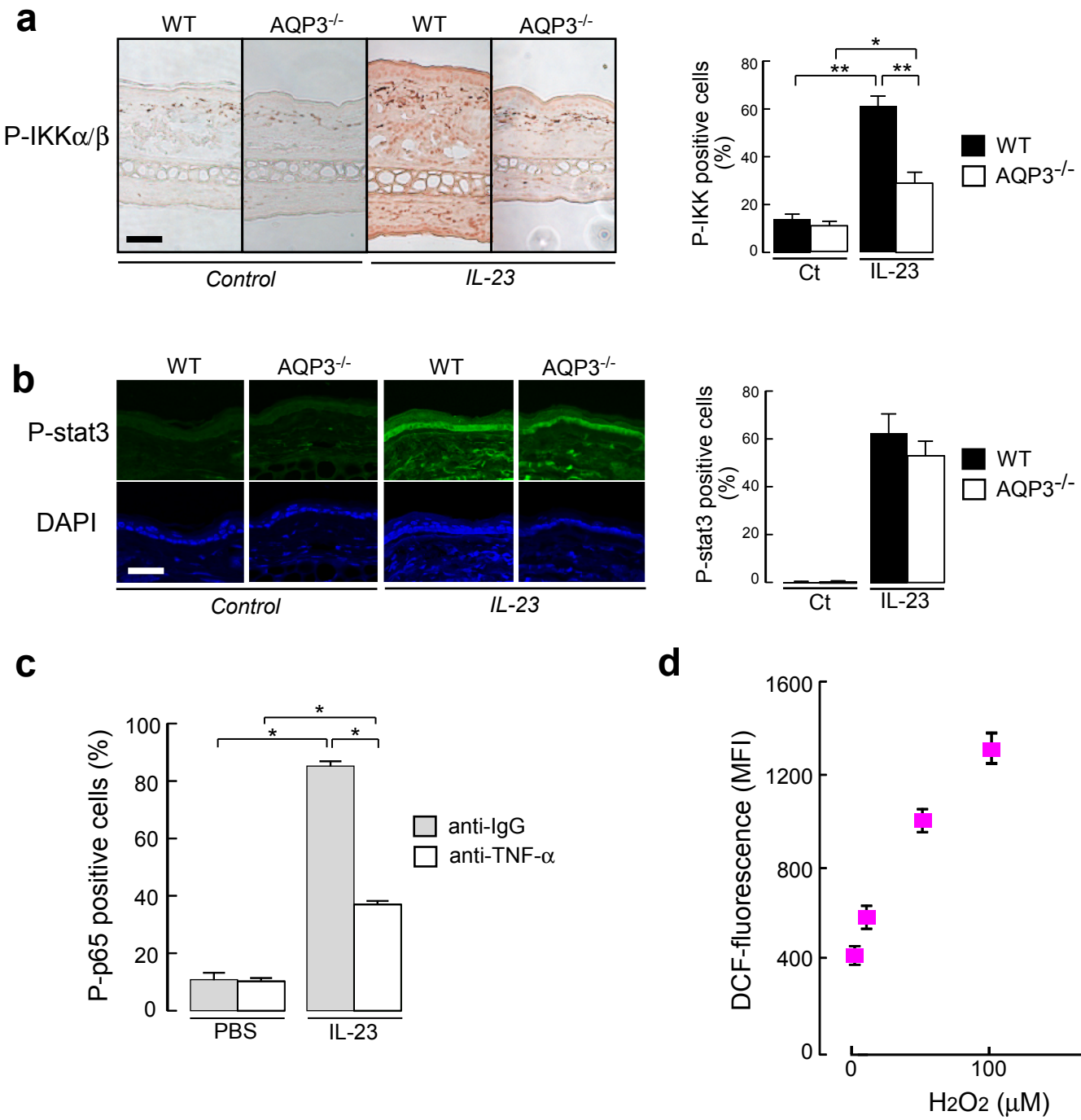

Supplementary Figure 3

a, b. IL-23 (500 ng) or vehicle control (PBS) was daily injected into the ear skin of WT and AQP3$^{-/-}$ mice intradermally for 4 days. The skin samples were excised at 24 hours after the final IL-23 injection. **a.** (left) Representative immunostaining with anti-phospho-IKKα/β and DAB. Bar, 100 μm. (right) The ratio of p-IKKα/β positive cells in the epidermis (SE, n=3, **p < 0.01, *p<0.05 by t-test). **b.** (left) Representative immunofluoresence of phospho-Stat3. Bar, 100 μm. (right) The ratio of p-Stat3 positive cells in the epidermis (SE, n=3) **c.** WT mice were treated daily with IL-23 or PBS in the presence of anti-TNF-α blocking monoclonal antibody or isotype control. Ratio of phospho-p65-positive cells in the epidermis shown in Fig. 3e (n=4, *p<0.01 by t-test). **d.** H_2O_2 solution (0-200 μM) in PBS was intradermally injected into the ear skin (40 μl/ear). Epidermal cells isolated by trypsinization were incubated with H_2DCFDA, and DCF fluorescence intensity was quantified by flow cytometry.

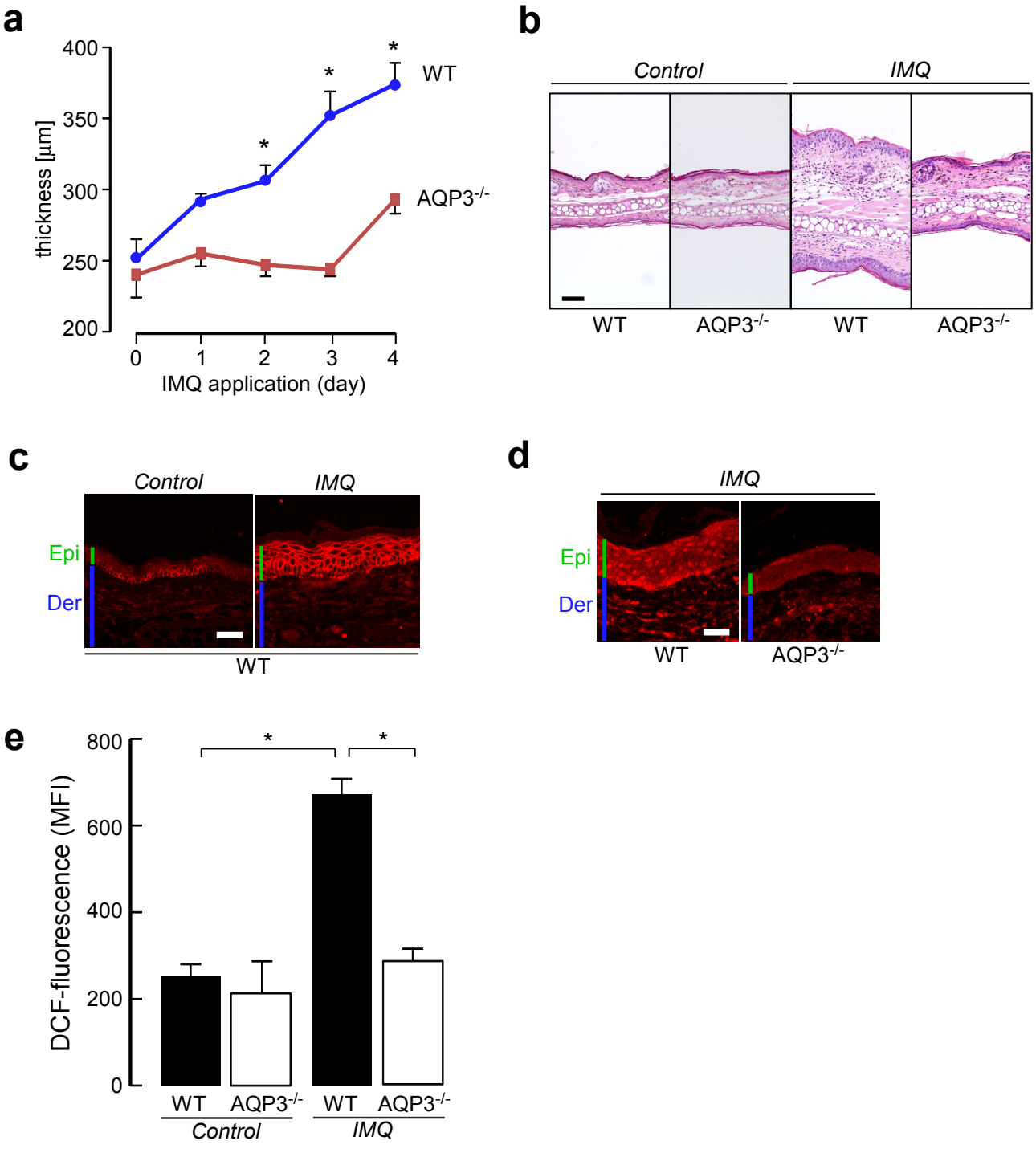

Supplementary Figure 4

Mice were treated daily with 10 mg of IMQ cream (5%, Beselna Cream; Mochida Pharmaceuticals, Tokyo, Japan) topically on the ear for 4 consecutive days. **a.** Ear swelling was measured with a micrometer (n=5-6, *p<0.01, WT *vs*. AQP3$^{-/-}$ by t-test) **b.** Hematoxylin and eosin staining of ears from WT and AQP3$^{-/-}$ mice. Bar, 100 μm. **c.** Immunostaining with anti-AQP3 antibody in WT mouse skin (red; AQP3). Bar, 50 μm. Epi; epidermis. Der; dermis. **d.** Immunostaining of phospho-p65 in IMQ-treated WT and AQP3$^{-/-}$ skin. Bar, 50 μm. **e.** Mean fluorescence intensity (MFI) of DCF fluorescence by flow cytometry analysis in epidermal cells from WT and AQP3$^{-/-}$ skin treated with IMQ (SE, n=5, *p < 0.01 by t-test).

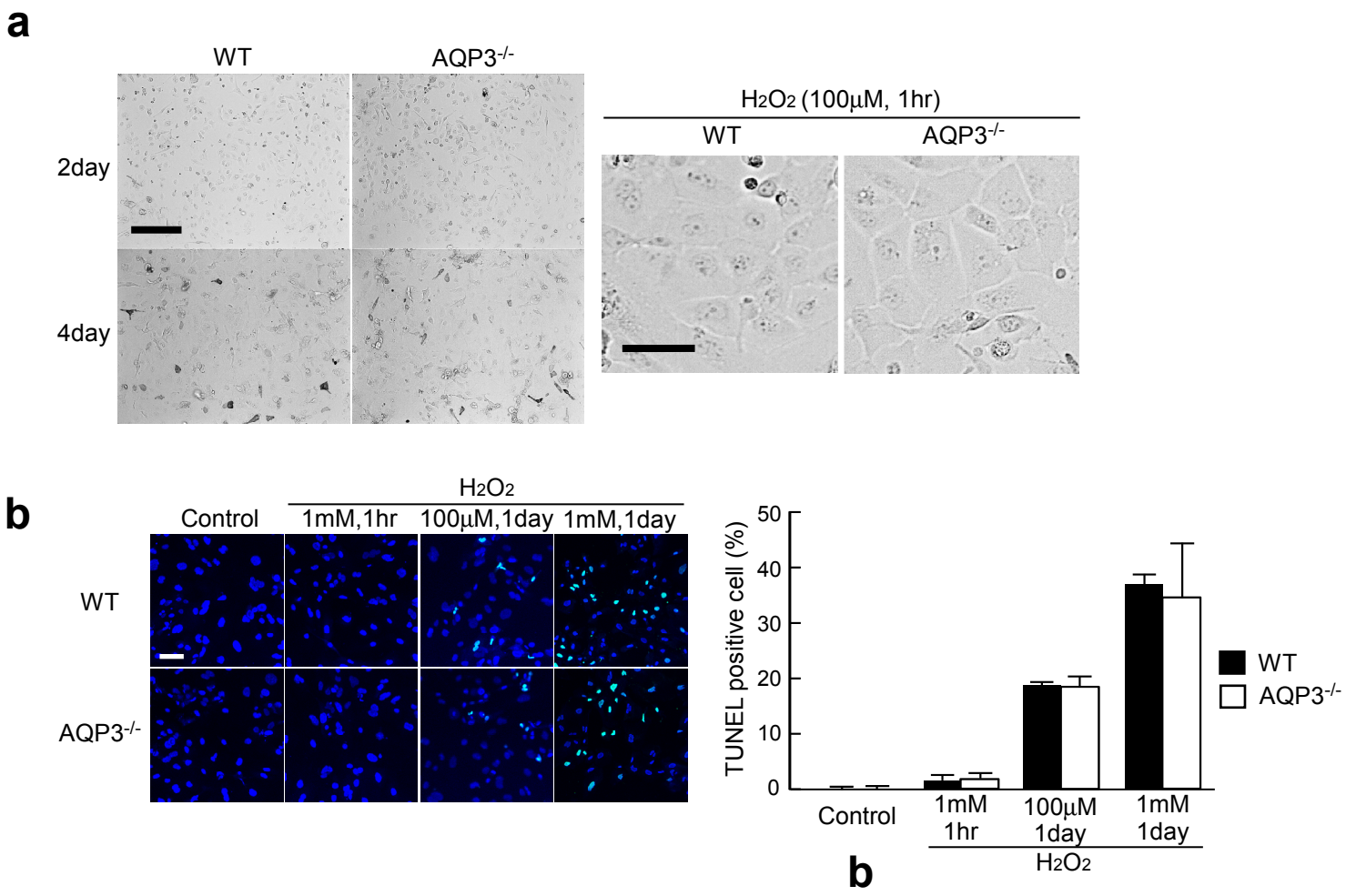

Supplementary Figure 5

a. Light micrographs of primary keratinocytes from WT and AQP3$^{-/-}$ mice at 2 and 4 days after plating, and at 1hr after incubation with H_2O_2 (100 μM). Left; bar, 200 μm. Right; bar, 50 μm. **b.** (Left) TUNEL staining of mice primary keratinocytes incubated with H_2O_2 (100 μM-1 mM, 1hr-1day). Green, TUNEL-positive cells. Blue, DAPI. Bar, 100 μm. (Right) Ratio of TUNEL-positive cells (over 100 cells from 2 different fields counted). **c.** WT mice primary keratinocytes were transfected with Nox1- or non-targeting (Ct) si-RNA. Cellular H_2O_2 levels determined by CM-H2DCFDA after TNF-α (100 ng/ml) stimulation (3 min, SE, n=5, *$p < 0.01$ by t-test).

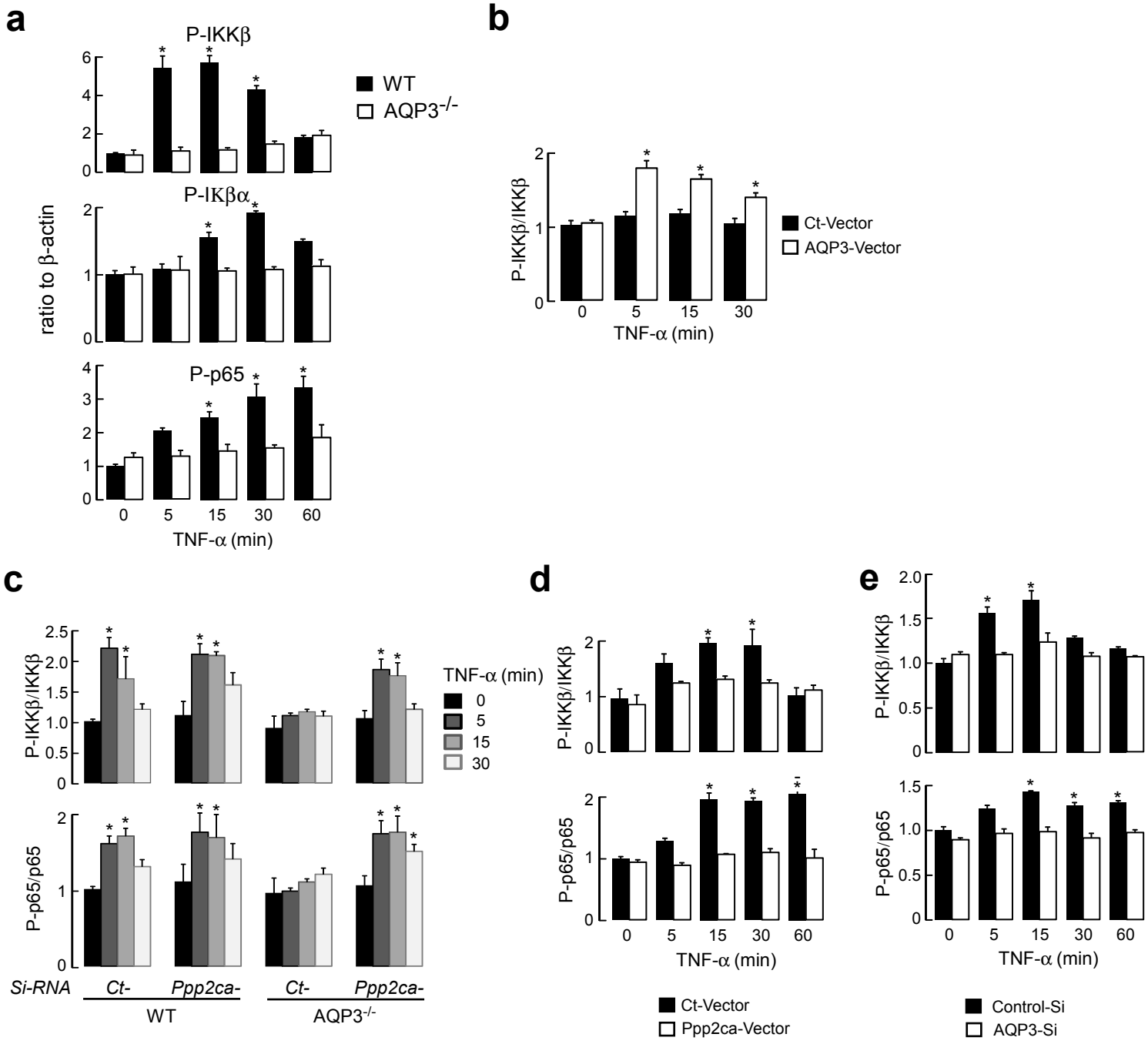

Supplementary Figure 6

Quantification of immunoblots.

a. P-IKKβ, P-Iκβα, and P-p65 were normalized to β-actin detected, from data as in Fig. 4a (SE, n=4, *p < 0.01, WT *vs.* AQP3$^{-/-}$). **b**. P-IKKβ was normalized to IKKβ, from data as in Fig. 6f (SE, n=3-4, *p < 0.01, control- *vs.* AQP3-vector transfected). **c-e**. The ratio of P-IKKβ to IKKβ and P-p65 to p65, from data as in Fig. 7d, Fig. 7g, and Fig. 8c (SE, n=3-4, *p < 0.01, TNF-α added *vs.* control cells in **c**, control- *vs*. Ppp2ca-vector transfected in **d**, control- *vs.* AQP3-SiRNA-transfected in **e,** by t-test)

Figure 3b

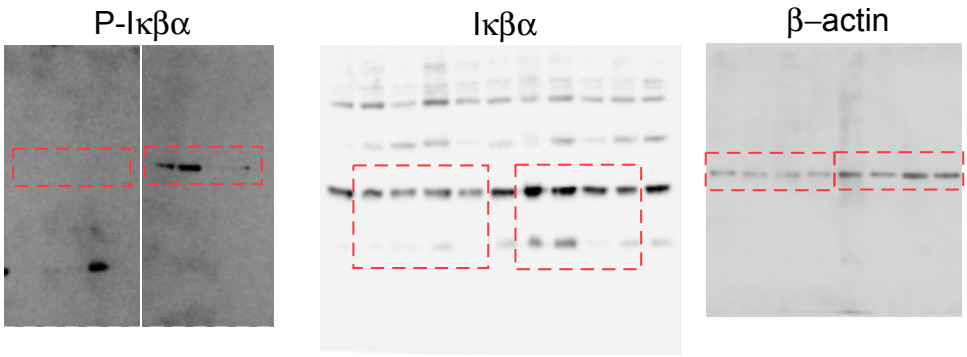

Figure 4a

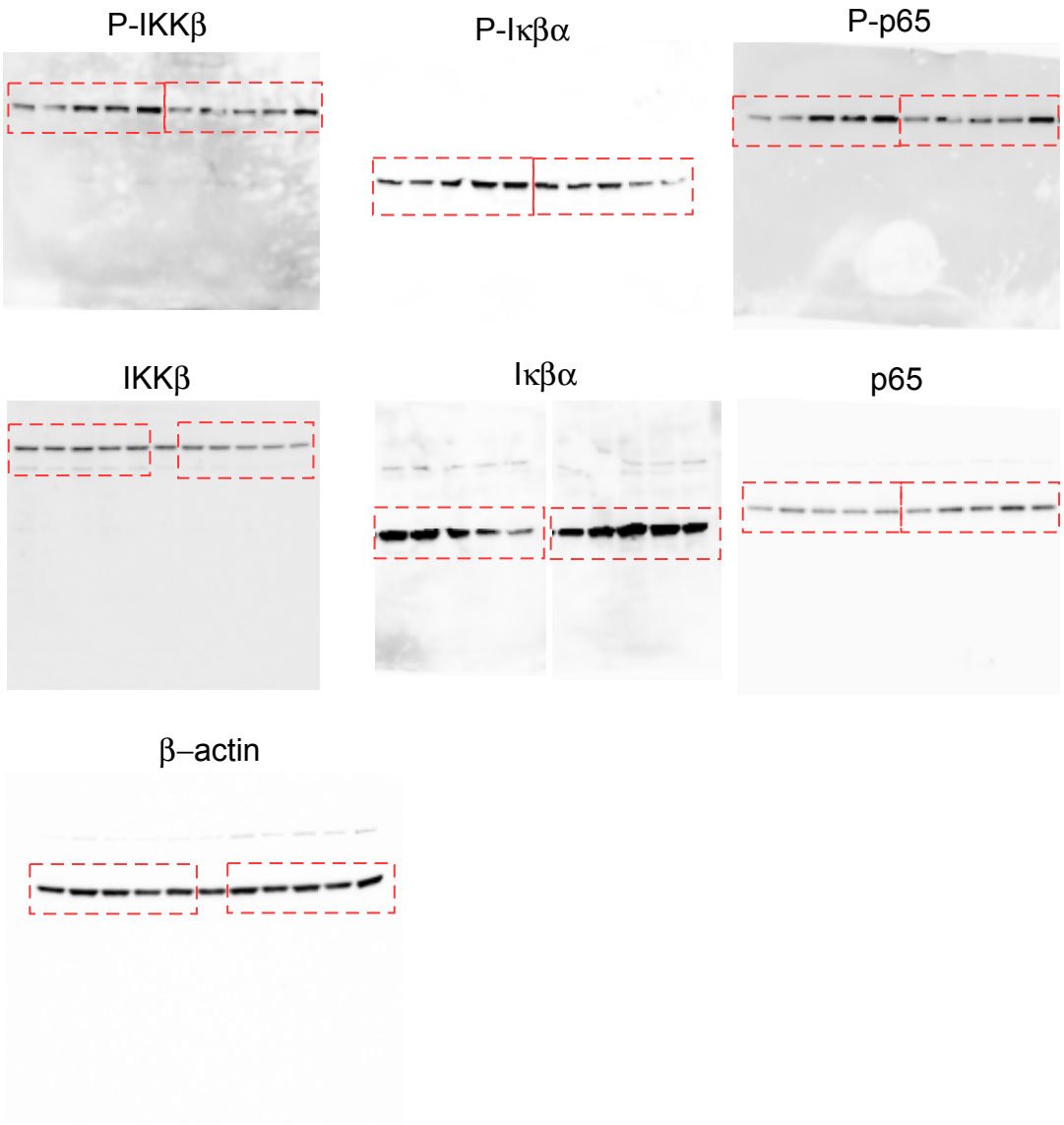

Supplementary Figure 7. Uncropped western blots (continued)

Figure 4b

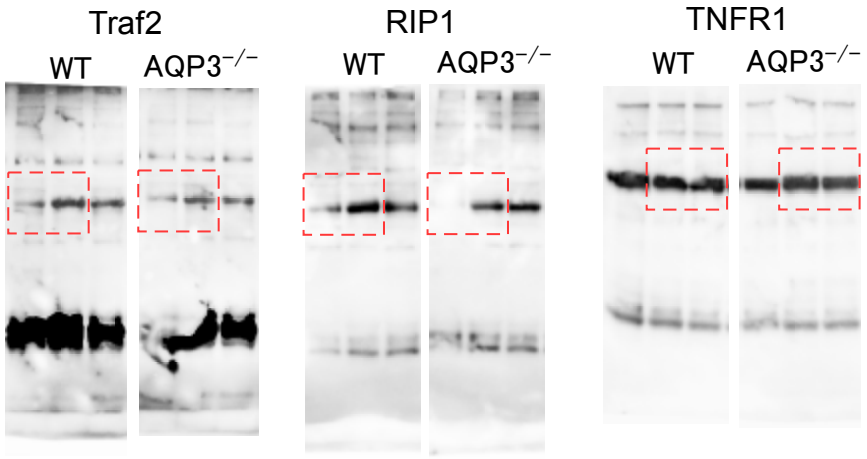

Figure 4d

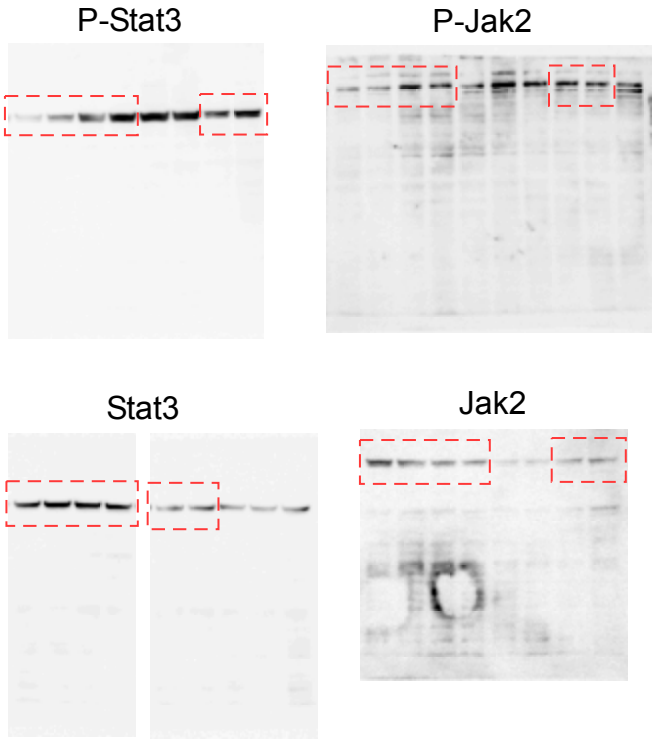

Figure 5g

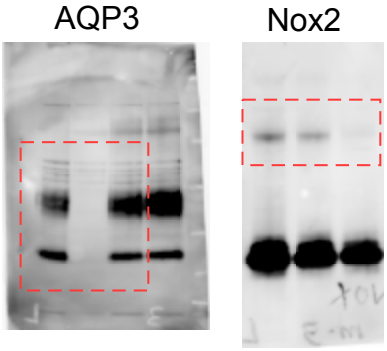

Supplementary Figure 7. Uncropped western blots (continued)

Figure 6c

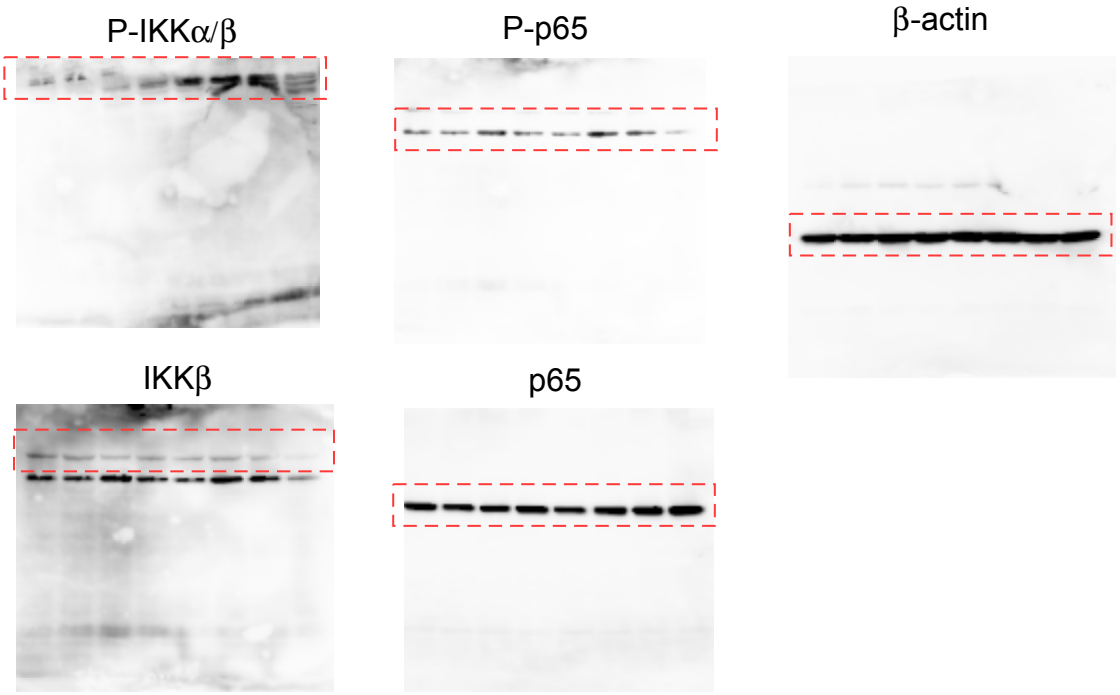

Figure 6d

Figure 6f

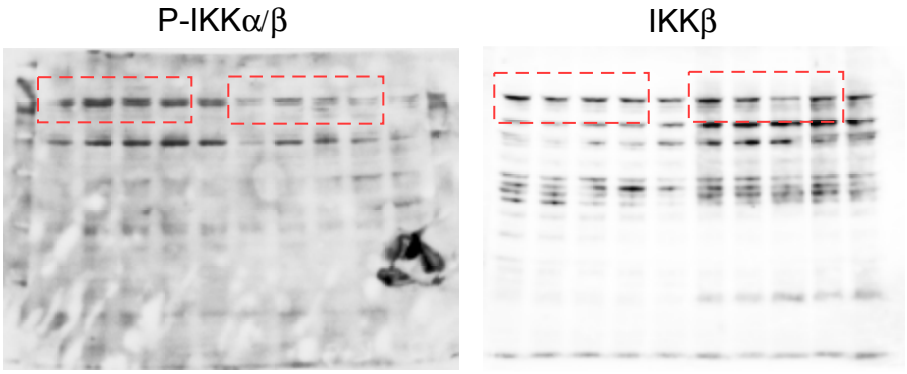

Figure 7b

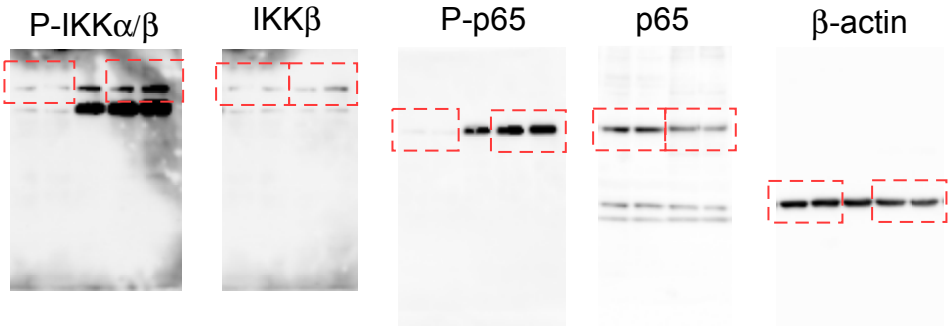

Supplementary Figure 7. Uncropped western blots (continued)

Figure 7c

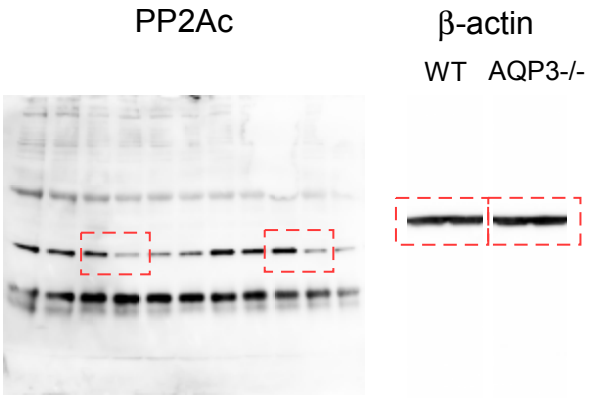

Figure 7f

Figure 7d

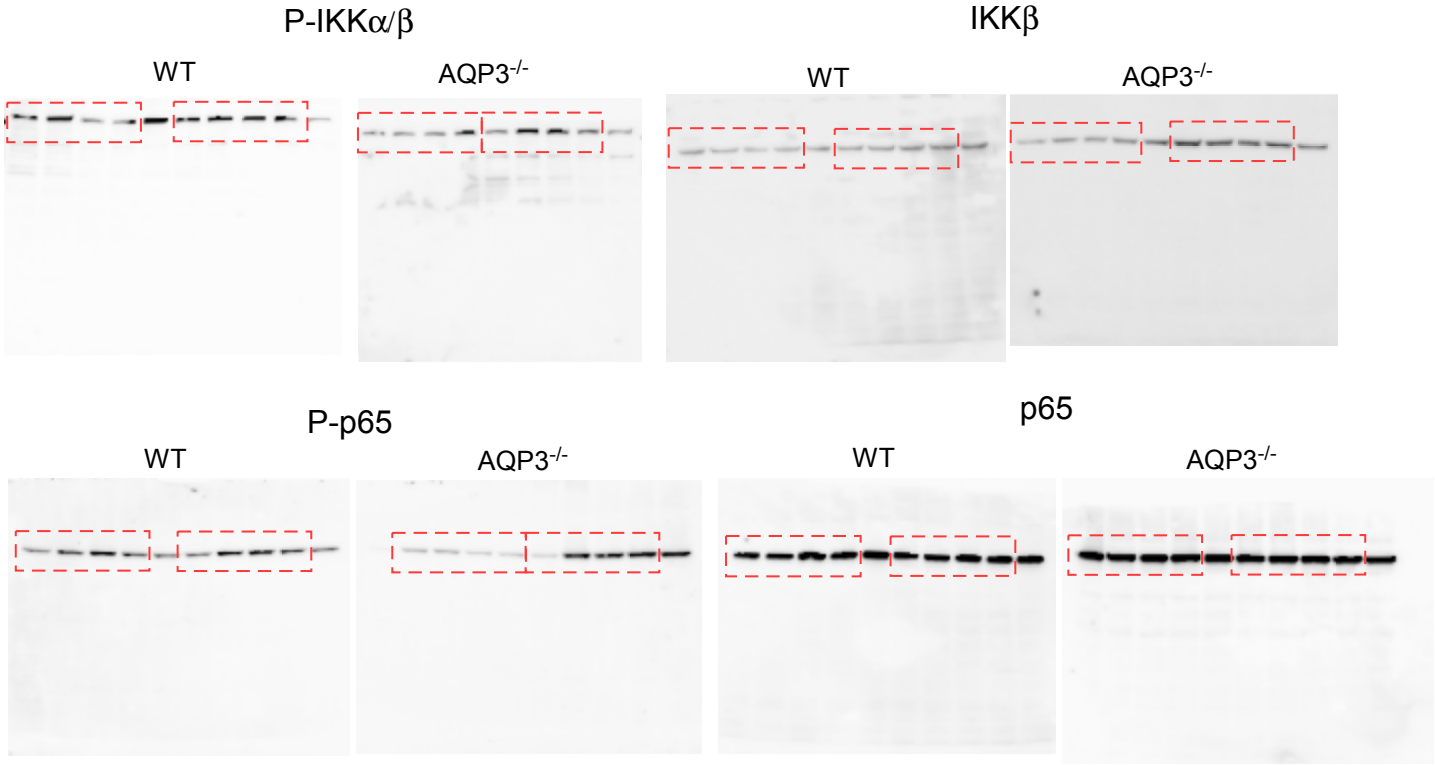

Figure 7e

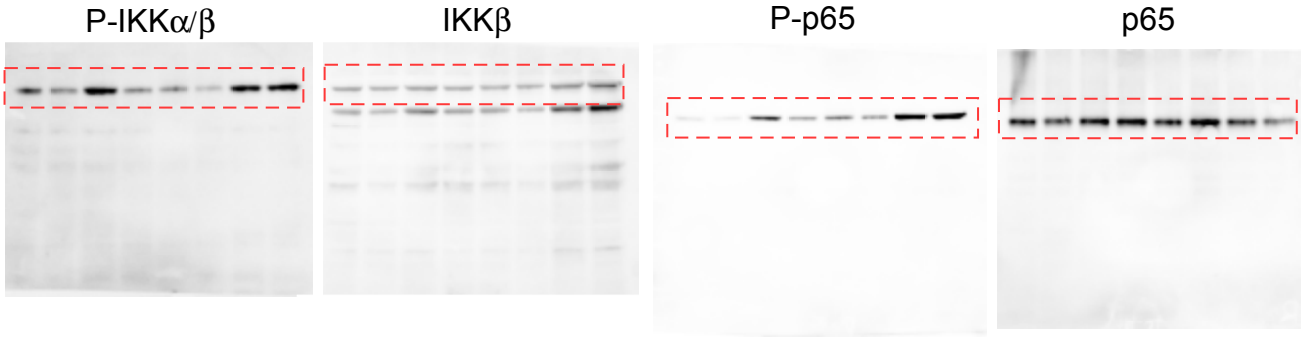

Supplementary Figure 7. Uncropped western blots (continued)

Figure 7g

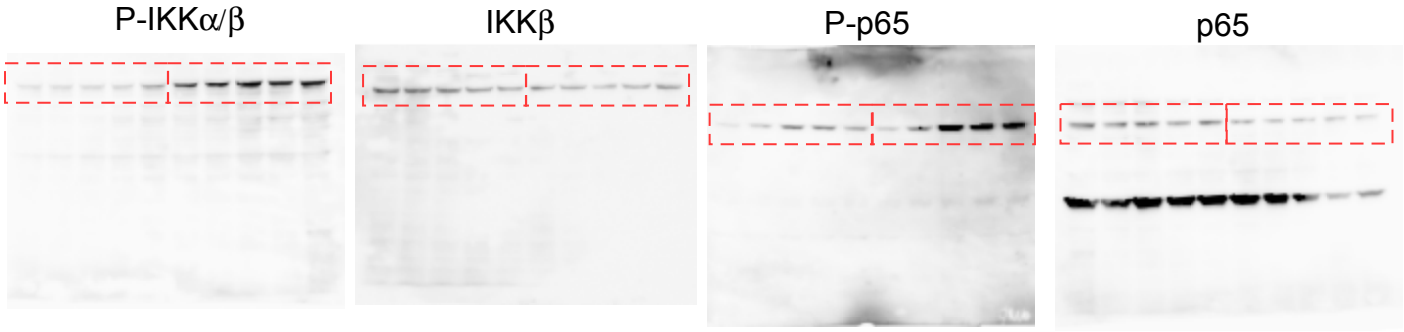

Figure 8a

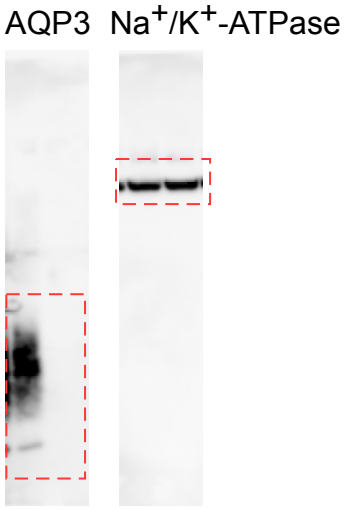

Figure 8c

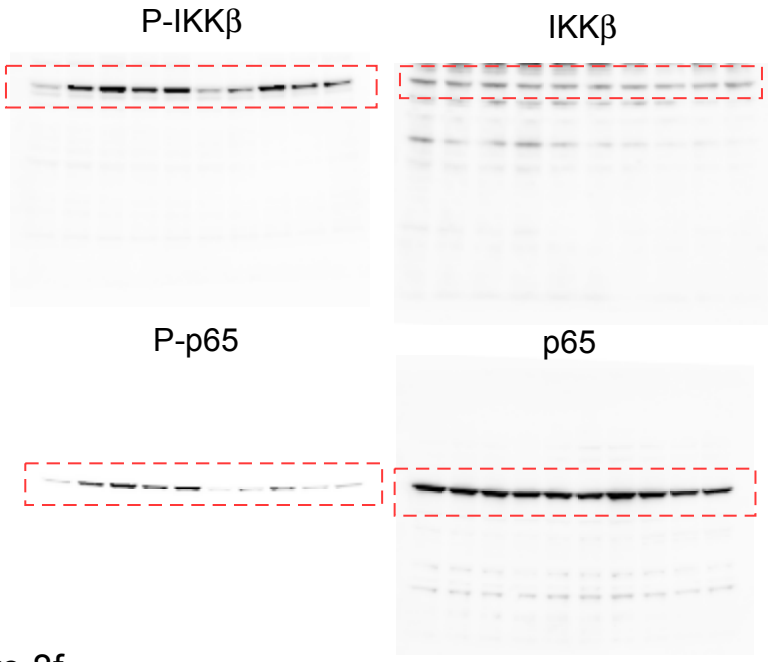

Figure 8e

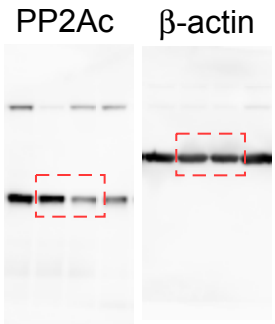

Figure 8f

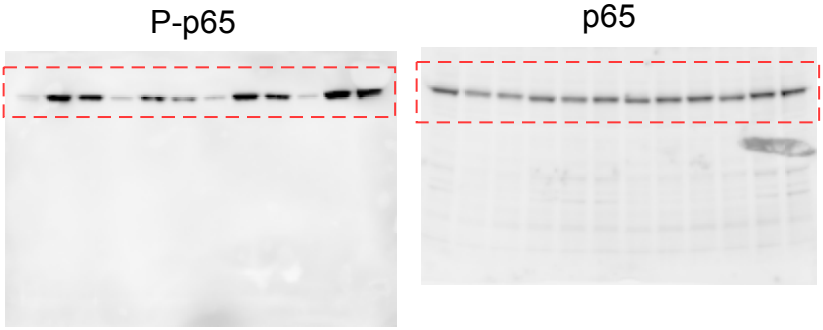

Supplementary Figure 7. Uncropped western blots

Supplementary Table 1. Primers for qRT-PCR analysis

Species	Gene	Forward/ Reverse	Sequence
mouse	IL17A	F	TCAGCGTGTCCAAACACTGAG
		R	GACTTTGAGGTTGACCTTCACAT
mouse	IL17F	F	ATGAAGTGCACCCGTGAAACAG
		R	CTCAGAATGGCAAGTCCCAACA
mouse	IL17C	F	CTCCTGCTTCTAGGCTGGTTG
		R	CCACCTGGCACTTCGAGTTAG
mouse	IL22	F	TTCCAGCAGCCATACATCGTC
		R	CTTCCAGGGTGAAGTTGAGCA
mouse	IL19	F	TGCAACTAGGATCATCCATGACAAC
		R	GATGATTCCTGTCAATCCAGGCTAA
mouse	CCR6	F	ATGCGGTCAACTTTAACTGTGG
		R	CCCGGAAAGATTTGGTTGCCT
mouse	CXCR3	F	GGTTAGTGAACGTCAAGTGCT
		R	CCCCATAATCGTAGGGAGAGGT
mouse	CCL20	F	ACTGTTGCCTCTCGTACATACA
		R	ACCCACAATAGCTCTGGAAGG
mouse	CXCL9	F	TCCTTTTGGGCATCATCTTCC
		R	TTTGTAGTGGATCGTGCCTCG
mouse	CXCL10	F	CCAAGTGCTGCCGTCATTTTC
		R	GGCTCGCAGGGATGATTTCAA
mouse	CXCL11	F	GGCTTCCTTATGTTCAAACAGGG
		R	GCCGTTACTCGGGTAAATTACA
mouse	CCL17	F	GACGACAGAAGGGTACGGC
		R	GCATCTGAAGTGACCTCATGGTA
mouse	CCL22	F	AGGTCCCTATGGTGCCAATGT
		R	CGGCAGGATTTTGAGGTCCA
mouse	CCL19	F	GGGGTGCTAATGATGCGGAA
		R	CCTTAGTGTGGTGAACACAACA
mouse	CCL21	F	GTGATGGAGGGGGTCAGGA
		R	GGGATGGGACAGCCTAAACT
mouse	CCL27	F	CCTCCCGCTGTTACTGTTG
		R	TTCCATGTGGACAATCCTCCT
mouse	S100A8	F	AAATCACCATGCCCTCTACAAG
		R	CCCACTTTTATCACCATCGCAA
mouse	Caspase3	F	TGGTGATGAAGGGGTCATTTATG
		R	TTCGGCTTTCCAGTCAGACTC
mouse	Ppp2ca	F	ATGGACGAGAAGTTGTTCACC
		R	CAGTGACTGGACATCGAACCT
mouse	AQP3	F	GCTTTTGGCTTCGCTGTCAC
		R	TAGATGGGCAGCTTGATCCAG
mouse	GAPDH	F	AGGTCGGTGTGAACGGATTTG
		R	TGTAGACCATGTAGTTGAGGTCA
human	IL17C	F	CCCTGGAGATACCGTGTGGA
		R	GGGACGTGGATGAACTCGG
human	IL6	F	ACTCACCTCTTCAGAACGAATTG
		R	CCATCTTTGGAAGGTTCAGGTTG
human	PPP2CA	F	CAAAAGAATCCAACGTGCAAGAG
		R	CGTTCACGGTAACGAACCTT
human	AQP3	F	TCTTTGACCAGTTCATAGGCAC
		R	GGCAGGGTTGACGGCATAG
human	GAPDH	F	ATGGGGAAGGTGAAGGTCG
		R	GGGGTCATTGATGGCAACAATA